Fabrication of Optical Stretchable Curvature Sensors with High Linearity

Bing Sun, Fei Li, Fanbo Feng, Kai Wan, Kaiming Zhou, and Zuxing Zhang

Abstract—**This paper presents an optical approach for fabricating stretchable curvature sensors that possess a high degree of reproducibility, can detect diverse curvatures, and can accommodate large strain ranges, while also being cost-effective and straightforward. The method involves the removal of the cladding and core of a single-mode fiber via a side-polishing technique, followed by encapsulation in a PDMS film with hundreds of micros. The resulting structure permits multimode interference effects that enable the sensor to exhibit high linearity and minimal hysteresis in its sensitive and reversible detection of bending deformations. Additionally, the unique mechanical and sensing properties of the sensor make it well-suited for integration into clothing or placement on skin surfaces to monitor a range of human activities, from subtle physiological signals such as wrist pulses to extensive motions involving joint bending and hand gestures.**

Index Terms—**Curvature, multimode interference, PDMS film, side-polishing.**

I. INTRODUCTION

The development of flexible and stretchable sensors that can fit to the contour and motion of the object has generated widespread interest in several fields, including geological survey [1-4], soft robotics [5-9], and biomedical science [10-11]. While electronic sensors rely primarily on changes in resistivity, conductivity, capacitive, and inductivity, these properties make them unsuitable for use in harsh environments and magnetic resonance imaging. Fiber-optic

Bing Sun, Fei Li, Fanbo Feng, Kai Wan, Zuxing Zhang are with the Advanced Photonic Technology Lab, College of Electronics and Optical Engineering & College of Flexible Electronics (Future Technology), Nanjing University of Posts and Telecommunications, Nanjing 210023, China (e-mail: b.sun@njupt.edu.cn; lifei_798@163.com; 1917540439@qq.com; wk09220330@163.com; zxzhang@njupt.edu.cn).
Bing Sun, Kaiming Zhou are with the Aston Institute of Photonic Technologies, Aston University, Birmingham B4 7ET, UK (e-mail: k.zhou@aston.ac.uk).

sensors, on the other hand, offer a promising alternative, as demonstrated by Wang et al., who successfully integrated an electrochemical SPR fiber-optic sensor into batteries for in situ chemical and electrochemical event detection without interfering with battery operation [12]. Flexibility and stretchability are crucial characteristics of sensors designed to measure curvature and strain through remote optical power spectrum measurements of light. While several strain measurement configurations exist, including FBG [13], LPFG [14], photonic crystal fiber [15], microfiber [16], Fabry-Perot microcavities [17], and others, their sensitivity is often limited by the range of measurement. For example, Liu et al. reported a high-sensitivity strain sensor based on an in-fiber rectangular air bubble, with a strain sensitivity of up to 43 pm/με but a measurement range limited to less than 500 με [18]. The limited deformability of optical fibers due to their stiff silica material constrains their use in stretchable sensors. However, the need for flexible and stretchable sensors with improved measurement range remains a pressing issue.

One potential strategy to address the challenges associated with pressure, strain, and bending sensing is to develop a stretchable waveguide, which can be fabricated by doping gold nanoparticles into a polydimethylsiloxane (PDMS) matrix [19]. The optical power loss in the waveguide can be measured to detect variations in these physical quantities. In addition, dye-doped PDMS optical fibers have been utilized for quantitative detection of tensile strains, which can be inferred from the corresponding absorption changes of light. Building on these ideas, a recent study by Li et al. introduced a soft and stretchable fiber optic sensor composed of a FBG inscribed onto a conventional glass optical fiber and a silicone film [20]. The FBG was embedded as a sinusoidal structure inside the silicone film, allowing for a 30% elongation in sensor length. Notably, this sinusoidal configuration confers stretchability to the sensor. Moreover, Yu et al. reported a highly sensitive and fast response optical strain sensor, which consisted of two evanescently coupled optical micro/nanofibers embedded in a PDMS film. This strain sensor demonstrated a gauge factor as high as 64.5 for strain values up to 0.5% and a strain resolution of 0.0012% [21].

Among various fiber structure schemes, D-shaped fibers have received widespread attention in the field of photonic sensing due to their simple structure, ease of manufacture, and cost-effectiveness. Of great significance, D-shaped fibers exhibit a propensity for facilitating multimode interference through the excitation of strong evanescent fields, thereby providing a versatile platform for the integration of various materials, including two-dimensional materials, photosensitive

materials, and specific biomaterials. In 2015, Zhao et al. reported the fabrication of a low-cost side-polished fiber with a rough polished surface, demonstrating strain and temperature sensitivities of up to -2.00 pm/με and 29.37 pm/°C, respectively [22]. In 2022, Sun et al. proposed a temperature-insensitive fiber refractometer based on a D-shaped no core fiber with a thin layer of PDMS film, exhibiting refractive index sensitivities of 140.1nm/RIU in the range of 1.32 to 1.37, and 1147 nm/RIU over a RI range from 1.38 to 1.44 [23].

The present study aims to utilize a coreless D-shaped single-mode fiber arrangement, which has been integrated into a polydimethylsiloxane (PDMS) film with varying thicknesses in the hundreds of microns, for the purpose of developing a curvature sensor. This sensor exhibits high sensitivity in detecting the direction of curvature and a broad dynamic range. The main interference guiding region, which comprises the ~5-mm-length core, is entirely eliminated. The proposed sensor demonstrates a measurement range of up to 6×10^{4} με and high sensitivity of 2.66 dB/m^{-1} with respect to curvature, thus enabling real-time monitoring of respiration, arm motion, and body temperature. The outstanding sensing performance, coupled with mechanical flexibility, highlights the potential of the proposed sensor for numerous photonic sensing applications.
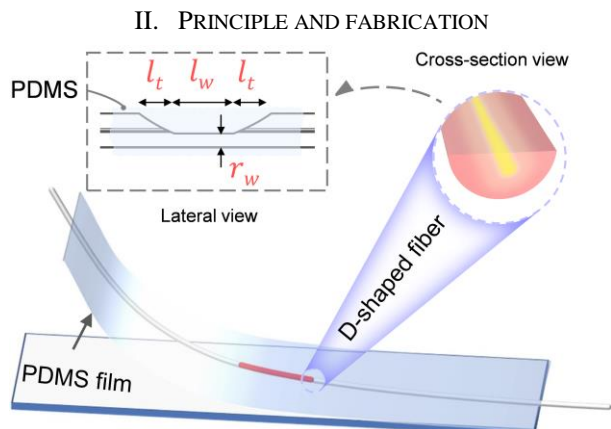
II. PRINCIPLE AND FABRICATION

Fig. 1 Schematic diagram of the three-dimensional configuration of the curvature sensor.

This study delineates the design of a novel fiber optic sensor that demonstrates stretchable attributes through the utilization of a polydimethylsiloxane (PDMS) film and a D-shaped fiber, where the PDMS film, measuring 0.6 mm×40 mm in size, houses a D-shaped fiber that is approximately 10 mm in length, as shown in Fig. 1. The fabrication process of the stretchable sensor entails the utilization of a dip coating method, wherein the PDMS solution is prepared through the mixture of two precursors of silicone elastomer and curing agent with a 10:1 ratio, followed by vacuum treatment for 40 minutes to remove bubbles. The dipping time and speed are optimized to encapsulate the D-shaped fiber within the well-designed PDMS film. Thus, the D-shaped fiber is centrally located within the PDMS film, as depicted in the inset, with a thickness of approximately hundreds of micros. Note that the

PDMS panel enables flexibility in curvature and strain measurements.

The removal of portions of the fiber cladding enables access to evanescent wave fields, and this can be achieved by employing a customized fiber side polishing technique. The efficacy of this method is largely determined by the degree of cladding removal, as illustrated by the inset diagram in Fig. 1. This diagram depicts the transitional (l_t) and residual areas (l_r), which exhibits similarities to a configuration described in a previous reference [24-25].
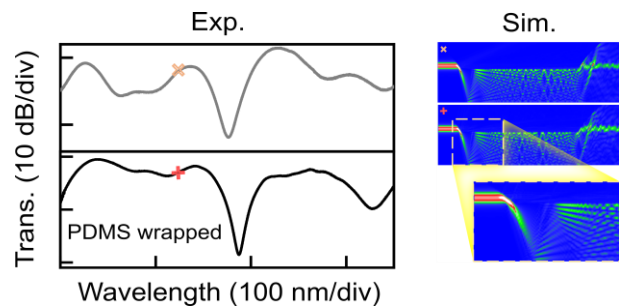

Fig. 2. (a) Measured transmission spectrum of the sample within/without the PDMS panel. (b) Beam propagation simulation.

The proposed sensing scheme operates based on modal interference theory, resulting in output light intensity exhibiting spectral maxima and minima. A beam propagation module is used to simulate the transmission spectra and field evolution of the D-shaped fiber, with the geometrical parameters including the length of the flat section ($l_r \sim 5$ mm), the lengths of the two transitional sections ($l_t \sim 2.5$ mm), the core refractive index of 1.4681, and the cladding RI of 1.4628. The core diameter was 9.0 µm, and the cladding diameter was 125 µm. Fig.2 (b) shows the simulated transmission light field along the optical fiber wrapped within/without the PDMS panel at the maxima wavelength, with an enlarged view of the curved polished surfaces of the transitional section providing deep insight into the multimode interference. The role of the employed PDMS film does prove to be of utmost significance in the conducted experiment. The exceptional optical properties stem from the refractive index characteristics of PDMS materials, which exhibit a low refractive index than that of silica, coupled with their compact dimensions, typically in the order of several hundred micrometers.

III. EXPERIMENT AND RESULTS

A sample with a residual thickness of $t_w \sim 50$ µm was fabricated. A broadband light source with a low polarization spectral range of 1250 to 1650 nm, with a degree of polarization smaller than 10%, was launched, while the transmission spectrum was recorded using an optical spectrum analyzer with a resolution of 0.02 nm.
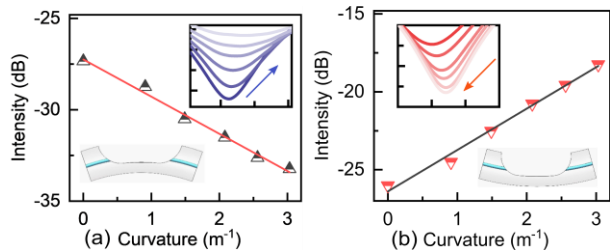
Fig. 3 (a) Spectral responses and the corresponding dip intensities of the sensor for the positive bending (a) and negative bending (b).

The bidirectional curvature sensing capability of a PDMS film integrated D-shaped fiber sensor was investigated, where the sensor was subjected to step-increased bending curvatures in both positive and negative directions. The output signals of the sensor showed opposite trends against the bending curvature. Note that the bent fiber was approximated as an arc of a circle, and the radius was used to calculate the sensor's curvature. During positive bending, the interference intensity increased with the rising curvature, while the opposite was observed during negative bending. The experimental results demonstrated the high sensitivity and linear response of the sensor. Specifically, the intensities of the dip increased with the curvature in the positive direction, and a high sensitivity of -2.04 dB/m^{-1} was obtained. The wavelength of the dip exhibited a slight change with the bending of the sensing section. Transmission spectra versus the negative curvatures were also analyzed, showing a corresponding sensitivity of 2.66 dB/m^{-1}. Such large dynamic range (more than 3 m^{-1}) for curvature sensing might be more useful in large infrastructures [26]. Moreover, these findings highlight the potential of the PDMS film integrated D-shaped fiber sensor for bidirectional curvature sensing applications.
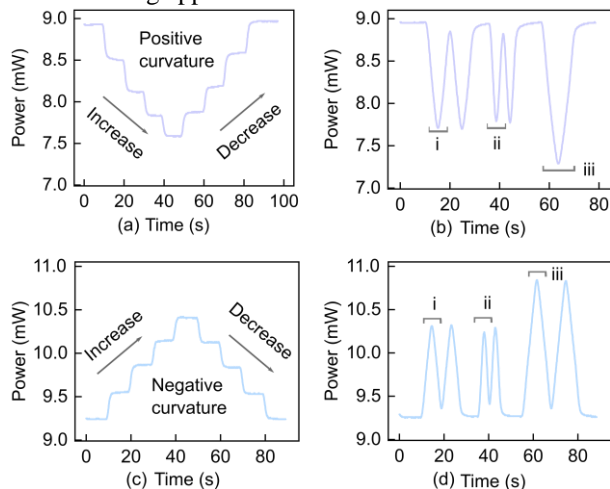
Figs. 4 (a) Response of the sensor to step-increased positive (a) and negative (c) curvatures. Dynamic response of the sensor to repeated cycles of positive (b) and negative (d) curvatures at different moving speeds and distances.

Based on the aforementioned static measurement experiments, a scheme was applied to detect dynamic bending by connecting one end of the sensor to a light source and the other end to a light detector. The bending state and the extent of bending were determined by measuring the change in optical power at the output. An external circuit controlled the stage, which moved at a uniform speed and changed curvature.

The experimental results of dynamic positive and negative bending were obtained and illustrated in Fig. 4 (a) and (c). The electric table paused for roughly 10 seconds each time it moved 2 mm, then returned to the initial state following an 8-mm-distance movement. The optical power decreased during positive bending, while it increased during negative bending, consistent with the static findings. Fig. 4 (b) and (d) respectively demonstrated the changes in different movement distances and different speed time power of the movement during positive and negative bending. Since the range of movement was identical for both states, the optical power variation was roughly the same. Furthermore, the movement time of state II was half that of state I, as the speed of State II was twice that of State I. When the movement speed remains constant, State 3 was found to elicit a comparatively reduced output owing to a greater degree of curvature resulting from a larger movement distance. This observation indicated a strong correlation between movement distance, curvature, and output level in State III. The utilization of the sensor in soft sensing applications is facilitated by its low cross-talk (strain and temperature) under curvature test conditions. These results suggest that this scheme can be used as a new solution for displacement sensing or speed sensing.
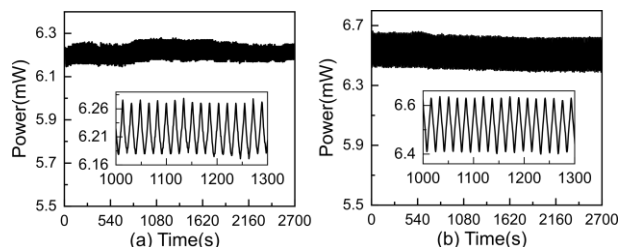

Fig. 5 (a) The optical power curve for 150 repeated bending cycles in the dynamic positive bending state. (b) The optical power curve for 150 repeated bending cycles in the dynamic negative bending state.

To evaluate the consistency and constancy of the curvature sensor, we executed a program to set the motorized stage's motion distance to 8 mm, followed by a return to the original position at an identical pace. This process was repeated for 45 minutes, subjecting the curvature sensor to 150 bending cycles. We used the experimental findings to illustrate the performance of the curvature sensor. The optical power curve for 150 repeated bending cycles in the dynamic positive bending state was presented in Fig. 5 (a), while Fig. 5 (b) displays the optical power curve for 150 repeated bending cycles in the dynamic negative bending state. The PDMS material's high flexibility and resilience provided effective protection for the D-shaped fiber, resulting in high stability and repeatability of the curvature sensor in both dynamic positive and negative bending states. Every coin has two sides. The utilization of a PDMS film-enveloped sensor induces hysteresis, thereby engendering a diminution in temporal response, a critical aspect in optical intensity detection, which necessitates rapidity.
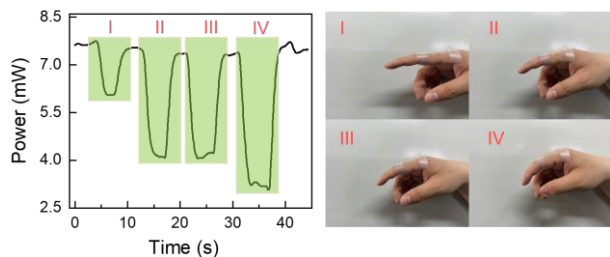
Fig. 6 Response of finger motion optical power over time. Bending state of finger.
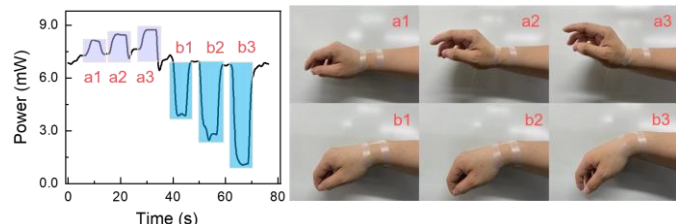

Fig. 7 Response of wrist motion optical power over time. Bending state of wrist.

We further investigate the applicability of the developed sensor for human motion monitoring by attaching it to the finger and wrist of the subjects. The experimental results, as presented in Fig. 6, depict the four bending states of the finger (I, II, III, and IV) and the corresponding increase in the bending amplitude, which leads to a reduction in the transmitted light power. This finding is in agreement with the previous experimental observations. Additionally, Fig. 7 demonstrates the change in transmitted light power of the sensor during wrist activity at different time intervals and compares the response of the wrist under various bent states.
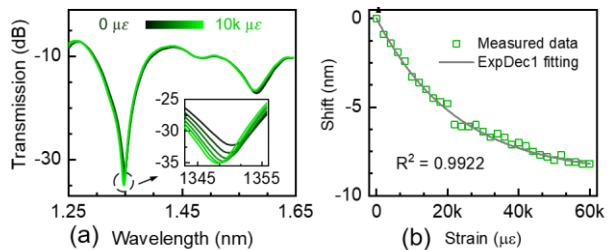

Fig. 8 (a) Response of transmission spectra under stretching. (b) Exp fit of stretch and release to center wavelength of dip in the range of 0~60000 με.

The stress sensing capability of sample #2 is demonstrated using an experimental device, as illustrated in Fig. 8, with a residual height of approximately 48 μm and length of about 8 mm. To alter the elongation of sample #2, the spacing between the two metal blocks is varied, thereby modifying the strain of the sample. The transmission spectrum of sample #2 under different levels of stress is presented. Specifically, Fig. 8 (a) depict the spectral changes during stretching over a strain range of 0-10000 με, with a tensile sensitivity of -0.21pm/με. The tensile response of the sensor in the range of 0~60000με is presented in Fig. 8 (b). Clearly, the amalgamation of the sensor with the flexible material PDMS significantly amplifies the stress detection range, attaining a noteworthy increment of approximately 60-fold in comparison to its counterpart lacking the PDMS film. Presently, the PDMS film manifests commendable ductility, thus endowing it with proficient buffering attributes.

Furthermore, the temperature response of a curvature sensor by placing it into a column oven (LCO 102 DOUBLE) with a temperature range of room temperature to 80 ˚C is investigated. The temperature measurement is conducted using a differential thermocouple (UNI-TUT320) with an accuracy of 0.1 ˚C. The temperature in the oven is increased gradually from 25 to 80 ˚C with a step of 10 ˚C, and then maintained for approximately 20 min during each temperature rise. The results demonstrate that the dip intensity induced by temperature is approximately 1.375 dB from 25 to 80 ˚C, indicating a low sensitivity of 0.025 dB/˚C, when compared with the response under curvature measurement [27]. This finding presents a novel approach for high-sensitive detection of curvature change while mitigating temperature cross-interference issues.

IV. CONCLUSION

In summary, we propose a curvature sensor that utilizes a D-shaped optical fiber wrapped with PDMS film for dual-parameter sensing of curvature and strain, achieved through intensity modulation. The proposed sensor effectively addresses the issue of cross-sensitivity between temperature and curvature, while enabling positive and negative differentiation of curvature, and a broad range of strain detection. Furthermore, we demonstrate the application of this sensor for real-time human movement detection and dynamic bending. The presented findings suggest promising potential for this sensor in diverse applications.

REFERENCES

[1] Lu X, *et al.*, "Experimental investigations on load transfer of PHC piles in highway foundation using FBG sensing technology," *International Journal of Geomechanics*, vol. 17, no. 6, Jun. 2017, Art. no. 04016123.

[2] Zheng Y, *et al.*, "Review of fiber optic sensors in geotechnical health monitoring," *Optical Fiber Technology*, vol. 54, Jan. 2020, Art. no. 102127.

[3] Hong, C.-Y., Zhang, Y.-F., Zhang, M.-X., Leung, L. M. G. and Liu, L.-Q., "Application of FBG sensors for geotechnical health monitoring, a review of sensor design, implementation methods and packaging techniques," *Sensors and Actuators A: Physical*, vol 244, no. 15, pp. 184-197, Jun. 2016.

[4] Kesavan, K., Ravisankar, K., Senthil, R. and Farvaze Ahmed, A. K., "Experimental studies on performance of reinforced concrete beam strengthened with CFRP under cyclic loading using FBG array," *Measurement*, vol. 46, no. 10, pp. 3855-3862, Dec. 2013.

[5] Guo, J., Zhou, B., Zong, R., Pan, L., Li, X., Yu, X., Yang, C., Kong, L. and Dai, Q., "Stretchable and Highly Sensitive Optical Strain Sensors for Human-Activity Monitoring and Healthcare," *ACS Appl Mater Interfaces*, vol 11, no. 37, pp. 33589-33598, Sep. 2019.

[6] Jiang, C., Zhang, Z., Pan, J., Wang, Y., Zhang, L. and Tong, L. "Finger-Skin-Inspired Flexible Optical Sensor for Force Sensing and Slip Detection in Robotic Grasping," *Advanced Materials Technologies*, vol. 6, no. 10, Jun. 2021, Art. no. 2100285.

[7] Zhu, H. T., *et al.*, "Self-Assembled Wavy Optical Microfiber for Stretchable Wearable Sensor," *Advanced Optical Materials*, vol. 9, no. 11, Jun. 2021, Art. no. 2002206.

[8] Zhang, L., *et al.*, "Ultrasensitive skin-like wearable optical sensors based on glass micro/nanofibers," *Opto-Electronic Advances*, vol. 3, no. 3, pp. 1-7, Mar. 2020.

[9] Pan, J., Zhang, Z., Jiang, C., Zhang, L. and Tong, L, "A multifunctional skin-like wearable optical sensor based on an optical micro-/nanofiber," *Nanoscale*, vol. 12, no. 33, pp. 17538-17544, Sep. 2020.

[10] Schmidt, E. J., *et al.*, "Electroanatomic mapping and radiofrequency ablation of porcine left atria and atrioventricular nodes using magnetic resonance catheter tracking," *Circ Arrhythm Electrophysiol*, vol. 2, no. 6, pp. 695-704, Dec. 2009.

[11] Tang, J., *et al.*, "Optical fiber bio-sensor for phospholipase using liquid crystal," *Biosens Bioelectron*, vol. 170, Dec. 2020, Art. no. 112547.

[12] Wang R, *et al.*, "Operando monitoring of ion activities in aqueous batteries with plasmonic fiber-optic sensors," *Nature Communications*, vol. 13, no. 1, 2022, Art. no. 547.

[13] Zhang, Y., Zhang, W., Zhang, Y., Wang, S., Yu, L. and Yan, Y., "Simultaneous measurement of curvature and temperature based on LP 11 mode Bragg grating in seven-core fiber," *Measurement Science and Technology*, vol. 28, no. 5, Mar. 2017, Art. no. 055101.

[14] Wang, S., Zhang, W., Chen, L., Zhang, Y., Geng, P., Zhang, Y., Yan, T., Yu, L., Hu, W. and Li, Y., "Two-dimensional microbend sensor based on long-period fiber gratings in an isosceles triangle arrangement three-core fiber," *Opt Lett*, vol. 42, no. 23, pp. 4938-4941, Dec. 2017.

[15] Yu Y, *et al.,* "Some features of the photonic crystal fiber temperature sensor with liquid ethanol filling," *Opt. Express*, vol. 18, no. 15, pp. 15383-15388, 2010.

[16] Li W, *et al.*, "High-sensitivity microfiber strain and force sensors," *Optics Communications*, vol. 314, pp. 28-30, 2014.

[17] Li, Jin, *et al*., "Microfiber Fabry-Perot interferometer used as a temperature sensor and an optical modulator," *Optics & Laser Technology,* vol. 129, 2020, Art. no. 106296.

[18] Liu S, *et al.* "High-sensitivity strain sensor based on in-fiber rectangular air bubble," *Scientific reports*, vol. 5, no. 1, 2015, Art. no. 7624.

[19] J. Guo, B. Zhou, R. Zong, *et al.*, "Stretchable and Highly Sensitive Optical Strain Sensors for Human-Activity Monitoring and Healthcare," ACS Appl. Mater. Interfaces, 11 (37) (2019), pp. 33589-33598

[20] Li T, *et al.*, "A Skin‐Like and Highly Stretchable Optical Fiber Sensor with the Hybrid Coding of Wavelength–Light Intensity," *Advanced Intelligent Systems*, vol. 4, no. 4, Dec. 2021, Art. no. 2100193.

[21] Yu W, *et al.* "Highly sensitive and fast response strain sensor based on evanescently coupled micro/nanofibers," *Opto-Electronic Advances*, vol. 5, no. 9, pp. 1-9, 2022.

[22] Zhao, J., Yin, G., Liao, C., Liu, S., He, J., Sun, B., Wang, G., Xu, X. and Wang, Y., "Rough Side-Polished Fiber with Surface Scratches for Sensing Applications," *IEEE Photonics Journal*, vol. 7, no. 3, pp. 1-7, 2015.

[23] Sun, B., Li, F., Xu, K., Zhou, K. and Zhang, Z., "Temperature-Insensitive Fiber-Optic Refractometer Based on Immobilization of Polydimethilsiloxane Film," *IEEE Photonics Technology Letters*, vol. 34, no. 3, pp. 165-168, 2022.

[24] He, C., *et al.,* "High performance all-fiber temperature sensor based on coreless side-polished fiber wrapped with polydimethylsiloxane," *Opt. Express*, vol. 26, no. 8, pp. 9686-9699, Apr. 2018.

[25] Dong, H., *et al.,* "Coreless side-polished fiber: a novel fiber structure for multimode interference and highly sensitive refractive index sensors," *Opt. Express*, vol. 25, no. 5, pp. 5352-5365, Mar. 2017.

[26] Y. Gong, T. Zhao, Y. -J. Rao and Y. Wu, "All-Fiber Curvature Sensor Based on Multimode Interference," IEEE Photonics Technology Letters, vol. 23, no. 11, pp. 679-681, June1, 2011

[27] F. Li, Y. Wen, K. Wan, F. Feng, B. Sun, and K. Zhou, "High-sensitive Intensity Modulated Curvature Sensor Based on D-shaped Fiber Wrapped in PDMS Film," in 27th International Conference on Optical Fiber Sensors, Technical Digest Series (Optica Publishing Group, 2022), paper W4.20.